Paper 107

©Civil-Comp Press, 2012
Proceedings of the First International Conference on
Railway Technology: Research, Development and Maintenance,
J. Pombo, (Editor),
Civil-Comp Press, Stirlingshire, Scotland

The Influence of Track Stiffness on the Measurement of the Wheel Rail Contact Force

A. Bracciali[1], L. Di Benedetto[1], F. Piccioli[1] and M. Cavalletti[2]
[1]Dipartimento di Meccanica e Tecnologie Industriali
Università di Firenze, Firenze, Italy
[2]VI-Grade s.r.l., Italy

Abstract

The measurement of loads acting on a railway line has become fundamental since the liberalisation of the access to the railway infrastructure (EC directive 440/91); in the years many design of track installation capable of measuring the vertical forces between wheel and rail have been developed. *Dipartimento di Meccanica e Tecnologie Industriali* of the University of Florence recently improved its reliable measurement system which is able to measuring the lateral (Y) force as well as the the vertical (Q) force at the wheel-rail contact while preserving mounting easiness. The system is based on the measure strains on the neutral axis of the rail by means of a set of strain gauges installed in a plug that is press fitted in a hole drilled in the rail web. As long as the reliable estimation of the average wheel-rail load requires the measurement and processing of the signals collected from a number of sensors, this paper investigates the influence of local track stiffness deviations on the quality of the estimation. A combined multibody-finite element approach is used to both overcome the limitations and get the advantages of the capabilities of the two methodologies.

Keywords: railway, track, stiffness, measure, contact force.

1 Introduction

The measure of rail strains in order to estimate the wheel-rail contact force acting during a train pass-by is a method which is used since several decades. The direct application of strain gauges on the rail, usually on the web, is well known and assessed but has some drawbacks, as long as it requires the work of an expert and certified operator and an amount of time and tools that are not easily available on site, especially if the installation has to be done on a railway line in service. For this reason, if direct application of strain gauges has to be used, a portion of rail is normally prepared in a laboratory and then welded in site on the portion of line under investigation. Maintenance nevertheless remains critical, inasmuch as any tamping or track operation may seriously harm the integrity of the measuring system which can only be restored at a large expense of resources.

The Dipartimento di Meccanica e Tecnologie Industriali of the University of Florence developed in the last decade a sensor which is capable to measure both vertical and lateral forces applied on the rail avoiding complicated operation on site (such as either bonding of strain gauges or cutting/welding of rails). Mounting is achieved by press-fitting an instrumented plug into a hole drilled in the rail web. The only operation required is therefore drilling holes with a standard rail drilling machine [1][2] (Figure 1).

The latest development consisted of splitting the sensor in two half-transducers, where each transducer is instrumented with a full-bridge strain gauges arrangement. When a vertical force Q is acting the bridges are both unbalanced with the same sign, while when a lateral force Y is acting the bridges are unbalanced with opposite signs (one with a positive and one with a negative unbalance). Clearly the average of the signals is proportional to Q while the difference is proportional to Y and thereby the system allows the recording of the effects separately [3].

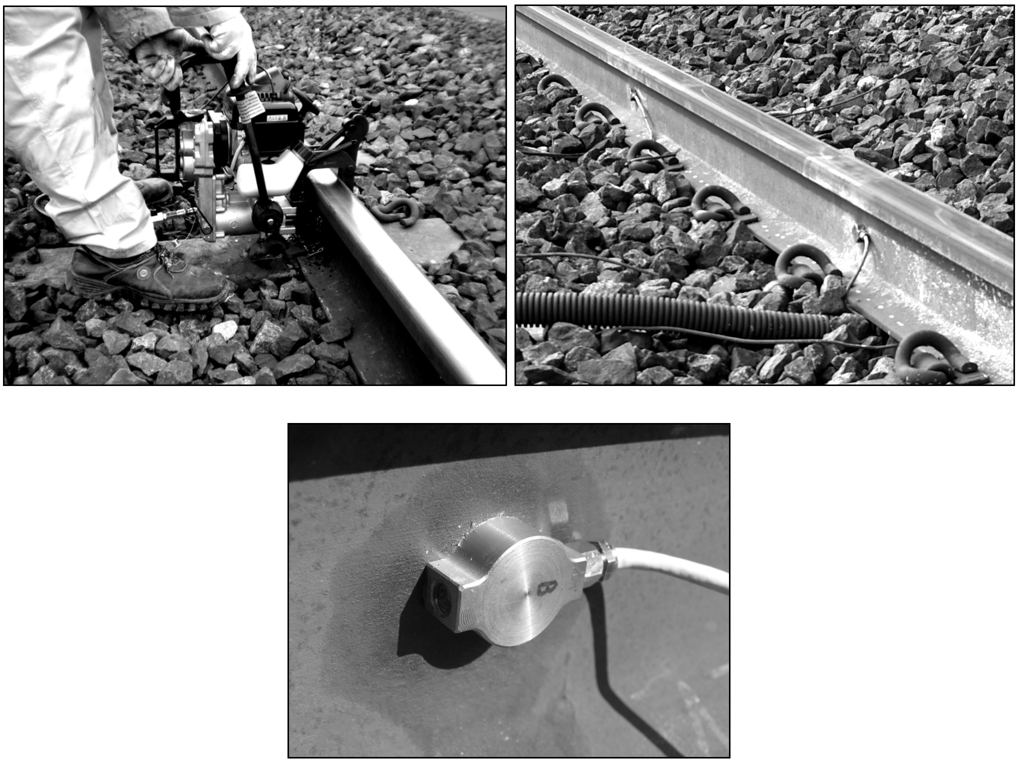

Figure 1: Mounting operations and final aspect of wheel-rail lateral and vertical force sensor (April 2011).

Two different configurations of the sensors were initially considered. In the first one strain gauges were bonded on each transducer at 90° (along the rail axis and orthogonal to it) and sensors were placed over the sleepers; in the second one strain gauges are bonded on each transducer with a similar arrangement but at 45° with respect to the rail axis and sensors were placed approximately at ¼ and ¾ of the sleepers span. The first configuration results in a higher strain concentration (better signal/noise ratio), the second one gives of a smoother and more flat signal (easier estimation of the peak). In this work only with the second configuration of the sensors will be analysed.

The success of any measuring system lies on its robustness, i.e. the capacity to cope with its mission regardless of the disturbances coming from external causes. For the system described in this paper there are several potential sources of "noise" which make less reliable the estimation of the force, affecting the theoretical distribution of the reaction of the track to lateral and vertical forces imposed by the wheel:

- possible irregularities in track tamping,
- dynamic behaviour (viscoelastic) o rail fastenings and ballast,
- dynamic vehicle response (coupling) when analysed together with the superstructure,
- speed variation of traffic over the monitoring station including a number of sensors.

In this paper the effect of the speed of the passing by vehicle is analysed thus trying to estimate the effects of inertia and damping on the value of strain signal measured, this will give an indication if it possible to implement the system on main line location instead of only yard location and if a speed correction of the measured signal is required.

This approach requires a combined multibody – FE approach. It is in fact evident that strains on the rail web are a local feature (consider that the internal diameter of the plug is 25 mm) while the solution of the multibody model has a much larger dimension --- the simulated track will be in the order of some hundred metres in order to dampen the transient results of the simulation. No FEM model can be done of such size, and moreover classical structural FEM models are not certainly adequate to simulate a multibody system; on the contrary, multibody packages by definition deal typically with lumped parameter systems and only in some cases, like the present one, with flexible bodies.

So, the simulations were conducted with a two-steps approach:

- first, a global solution including the deflections of the rail during pass-by of a train under different conditions (speed, tamping defects, etc.) will be searched for by the use of a multibody commercial package;
- then, the solution obtained with the multibody software will be introduced as a boundary condition to a detailed – but quite limited in size – linear structural FEM model of the rail in order to derive local strains and, therefore, the "readings" of the sensors.

2 Multibody model of track and vehicle

In order to simulate the coupled behaviour of the vehicle and of the infrastructure it is necessary to make use of an approach which can take into account the dynamic behaviour of both a vehicle and the track. Without making use of this approach it is quite likely to miss the effect of vehicle suspensions and of local track features.

Instead of developing an *ad hoc* mathematical model, which was outside the scope of this research, a multibody software package was used to model the vehicle and the track and their interaction.

The package *VI-Rail*, the software extension for *MSC ADAMS* specific for rail simulation, has the unique feature of offering an internal plug-in, called *Flextrack*, which is capable of describing a flexible track allowing to set the rheological parameters for rail fastenings and sleeper (stiffness and damping) as well as the inertial properties of rails, sleepers and ballast [4]. By using this tool the parameters of a track can be tuned according to experimental results and forces and displacements in a specific point of the track can therefore be simulated and analysed. It is important to underline the *Flextrack* permits to define track parameters for different parts of the track (down to a single sleeper) allowing to define a simulated track with quasi-continuously varying parameters which continuously interacts with a running vehicle, a feature that can be hardly realized by using mathematical approaches.

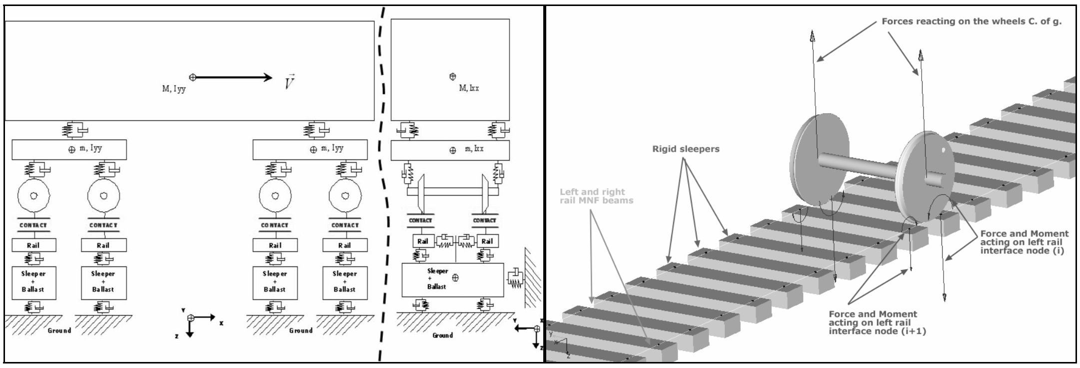

Figure 2: The general multibody definition of a vehicle and track within *VI-Rail* software package (left); definition of output track parameters in the *Flextrack* module (right). The wheel-rail contact module shown on the left is included in the basic *VI-Rail* package.

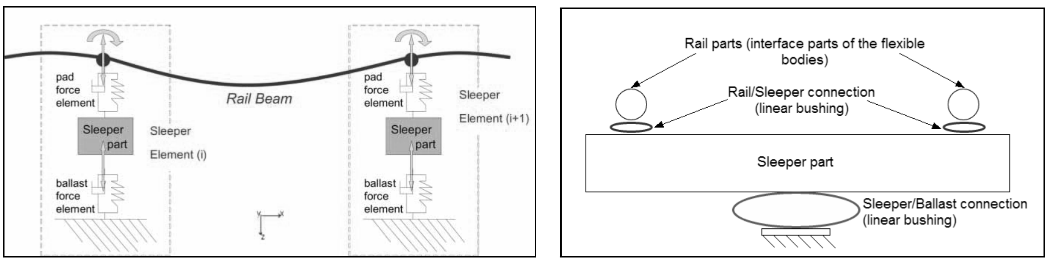

Figure 3: Rheological model of the flexible track as defined in the *Flextrack* option.

Each mass is connected by linear visco-elastic suspension according to Voigt model. In particular, sleepers are considered as rigid masses with three degrees of freedom for the vertical displacement, lateral displacement, and roll rotation. Pads and fastenings are schematized with force elements to attach the rails at each interface node situated above every sleeper. Two identical connections force elements are created per sleeper to connection to ground.

A standard rail type 60E1 according to [5] (mass 60 kg/m, section area 7668 mm^2, moments of inertia 30383788 mm^4 and 5120777 mm^4) was used supported by 300 kg monobloc sleepers. The rheological parameters used in the simulations of flexible track are listed in Table 1, although only some results will be shown in this paper. To simplify the interpretation of the results, the convention indicated in Table 2 will be used throughout the rest of the paper.

Object	Direction	Stiffness	Damping
Pad	Vertical	k_{pv}= 150-50 kN/mm	k_{pv}=350-250-125 kNs/m
	Lateral	k_{pl}= 280 kN/mm	k_{pl}= 58 kNs/m
	Roll	k_{pr}= 800-270 kN/rad	k_{pr}= 390 Ns/rad
Ballast	Vertical	k_{bv}= 160-80 kN/mm	k_{bv}= 360 kNs/m
	Lateral	k_{bl}= 120 kN/mm	k_{bl}= 40 kNs/m
	Roll	k_{br}= 130-65 kN/rad	k_{br}= 290 kNs/rad

Table 1. Rheological parameters used in the simulations. All ballast quantities are referred to the whole sleeper.

Track definition	Ballast Vertical Stiffness k_{bv}	Pad Vertical Stiffness k_{pv}
average track	k_{bv}= 160 kN/mm	k_{pv}= 150 kN/mm
soft ballast	k_{bv}= 80 kN/mm	k_{pv}= 150 kN/mm
soft pad	k_{bv}= 160 kN/mm	k_{pv}= 50 kN/mm

Table 2. Definition of track properties.

All simulations used the *Flextrack* model for at least a part of the track that was simulated with the main aim of taking into account the stiffness under each single support. A passenger car, described below, ran on a 375 m-long straight track, made of a 210 m rigid section followed by a 150 m flexible section ending with a further 15 m rigid section. Tests were made at different speed in order to evaluate the influence of track parameters on the contact force and on the sleeper reaction force.

As long as this study is more related to track behaviour than to vehicle behaviour, and it is not linked to a specific kind of vehicle, a coach available in the software library ("Manchester passenger wagon") was used for simulations as a "benchmark vehicle". This vehicle is well known in literature and allowed to perform all the following analysis excluding modelling error of the vehicle ensuring at the same time the possibility of repeating the analysis by any *VI-Rail* user. Nevertheless the vehicle is well representing an average two-bogies passenger wagon and the analyses conducted here keep their validity.

3 Finite element model of the rail and transducer

As the output parameter that has to be analysed for the evaluation of the transducer is the strain on the surface of a hole drilled in the rail, a linear elastic finite element of the track was developed. Actually, two separate models were developed:

- a first model capable of using directly the output of the multibody simulations;
- a second one, a bit more detailed, used for quasi static evaluations.

In both cases the aim of the model was the evaluation of the strain in the transducer when the wheel, or the force representing the wheel, travelled along a stretch of rail.

3.1 Model for dynamic evaluation

When the full non-linear dynamics of the track interacting with the vehicle is taken into account, a direct FEM solution is computationally very expensive and almost impracticable. For this reason the deformations obtained by the use of the multibody package described above were imposed to the FEM model (made with ANSYS 13.0) of the rail equipped with sensors.

As long as the output of the multibody is currently available only as the vertical displacement of the rail axis in correspondence of the sleepers for each time step, an approximation was adopted by assuming that the reciprocity theorem (certainly valid in the case of a continuous support of the rail) holds also for the discrete supports case.

For each simulation, the vertical deformation of the neutral axis of the rail was saved when the leading wheel of the vehicle was at a certain distance from a given sleeper. This operation was repeated every 100 mm along the route, thus obtaining the "operational travelling deformation" of the rail. Then the vertical displacement of an arbitrary point along the rail axis (obviously including those where sensors are located) was obtained by shifting the rail displacement curve over a sleeper by the distance between the desired point and the sleeper (see Figure 4).

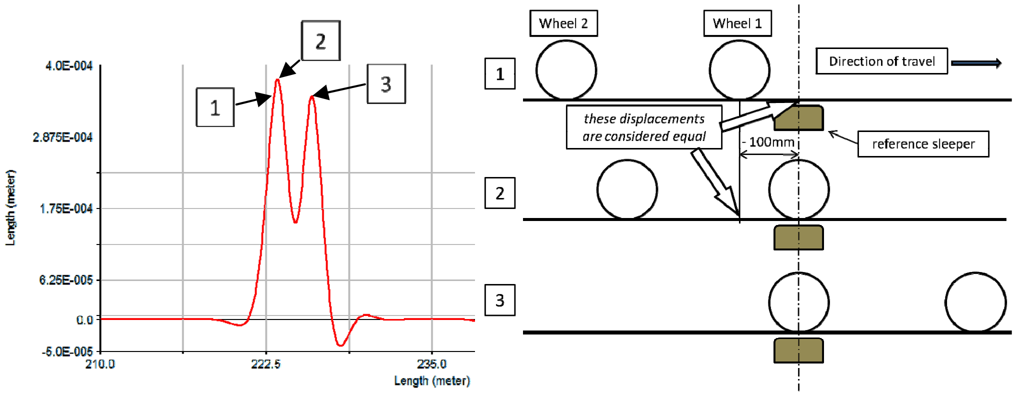

Figure 4: The displacement of a point at a given distance (e.g. 100 mm) from the sleeper when the wheel is on the sleeper was retained equal to the displacement of the sleeper when the force is acting on that point. Left: typical vertical displacement of the rail axis. Right: the actual bogie positions corresponding to the points indicated on the left.

In the finite elements model the axis of a “free” rail was deformed with an imposed displacement corresponding to the load acting as result of the wheel passage (Figure 5). Displacements were given every 50 mm to a model with a mesh with 15 mm size (2 mm in the transducers area), resulting in a model with 506465 elements.

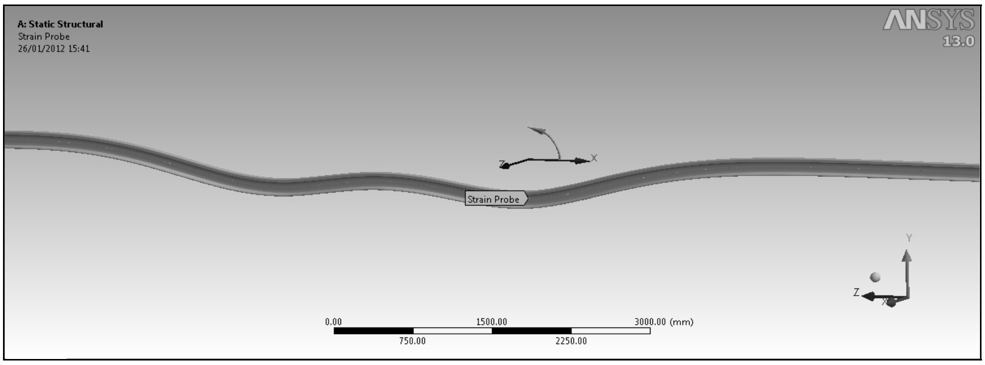

Figure 5: Instantaneous vertical deflection of rail in the FEM model after *VI-Rail* deflection data application

3.2 Model for quasi-static evaluation

In order to validate the behaviour of the dynamic model with the speed and also to investigate the influence of some aspects neglected in the previously described model, a model for quasi-static evaluations was built. In this model the following aspect were introduced:

- finite width of the sleeper support,
- strains in the rail section considered as a 3-D elastic body.

For this model 20 sleepers were simulated with a spacing of load application points of 50 mm (25 mm close to sensors position). Mesh size was retained similar to the previous case (18 mm far from the sensors and 2 mm in the sensors area) with a total of 289703 elements (Figure 6).

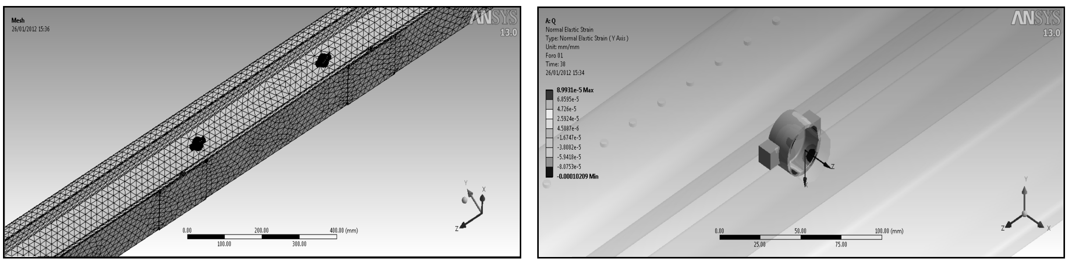

Figure 6: Mesh of the static model in the transducer area (left) and an example of a typical output (strains on one sensor) (right)

In this model loads are applied directly with forces on the railhead, while rail foot vertical supports consider the equivalent stiffness of railpads and ballast in series. In this way equilibrium conditions are satisfied (the set of externally applied is the same) but congruence may not, as long as the *distribution* of forces may be different (pressures instead of localized force, for example in the case of sleepers). This effect can be retained as local and non influencing the global behaviour of the vehicle and the track. In other words, overall boundary conditions obtained with lumped constraints parameter are compared to the results of a detailed FEM model where constraints are modelled with their finite size.

In order to evaluate the behaviour of the model previously described that uses *VI-Rail* input data of sleeper deflection, a comparison at standing (static load) was performed. The longitudinal strain in the centre of the rail foot at mid span between sleepers was used as reference parameter, for the dynamic model the quasi static value was extrapolated from the response at various speeds. The difference between the two models is in the order of 14%, that can be explained by both the difference in the rail support (finite size vs. point) and the fact that *VI-Rail* uses Euler-Bernoulli beams for the model of the rail while the 3-D static model of the rail is much likely to behave as a less stiff Timoshenko beam (Figure 7).

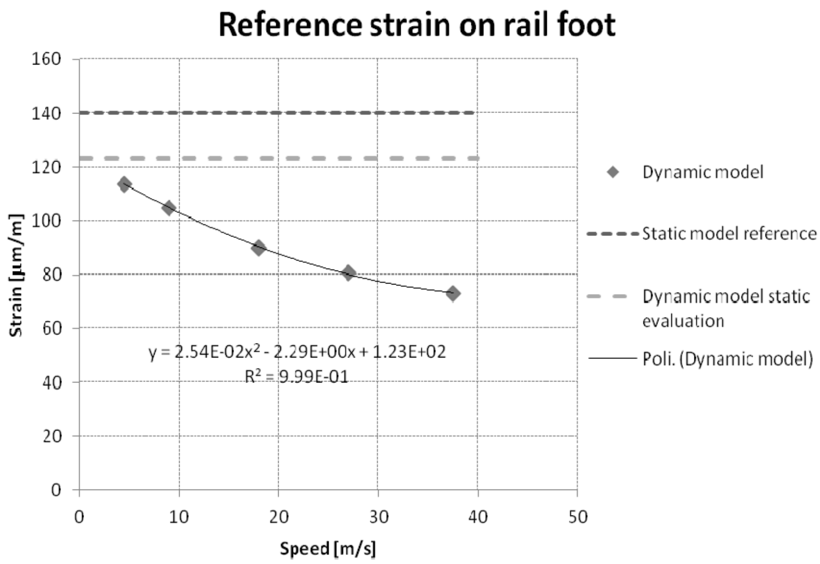

Figure 7: Comparison of dynamic (i.e. using *VI-Rail input*) and static evaluation of reference strain on rail foot.

When looking at the strain signals in the transducers the difference between the static and the "dynamic" model is much higher than when looking at the rail foot. This is believed to be due to the two previously mentioned effects (finite sleeper/pad surface and rail section compression) that cause different strain field and strain concentration in the holes.

4 Results and discussion

In this section the results of the analysis are discussed looking at the influence of stiffness, damping and speed on sleeper reaction forces, on wheel-rail contact forces and on sensors output (in terms of strain).

4.1 Effects of speed on wheel-rail contact force

The first analysis performed was about the contact force between wheel and rail, extracting from multibody simulation the values of the average (static) and fluctuating (dynamic) components of wheel-rail contact forces.

It should be pointed out that although the time step in the multi body simulation was Δt=1 ms (f_s=1 kHz), no defects were present on the wheel (which was perfectly round) and on the rail (which was perfectly flat). The dynamic contribution to the contact force is therefore only due to the parametric excitation given by the discrete and regular pattern nature of the support of the rail (i.e. sleepers) and any other high frequency content (as given in practice by rail roughness and wheel out-of-roundess) is not present.

As an example Figure 8 shows the time history of the wheel-rail contact force with the vehicle travelling at 18 m/s (64.8 km/h), where the dynamic part of the force, which is barely around 100 N vs. a static force of 54.65 kN, can be observed for different stiffnesses of pads and ballast

Figure 9 shows the static and the dynamic part of the contact force for a tangent track with speeds in the range 4.5 to 37.5 m/s. As expected the static part is not influenced by speed, while the dynamic part is instead increasing with speed; also the very small influence of the pad and ballast stiffness (at last in the range investigated) is visible both for the static and the dynamic part

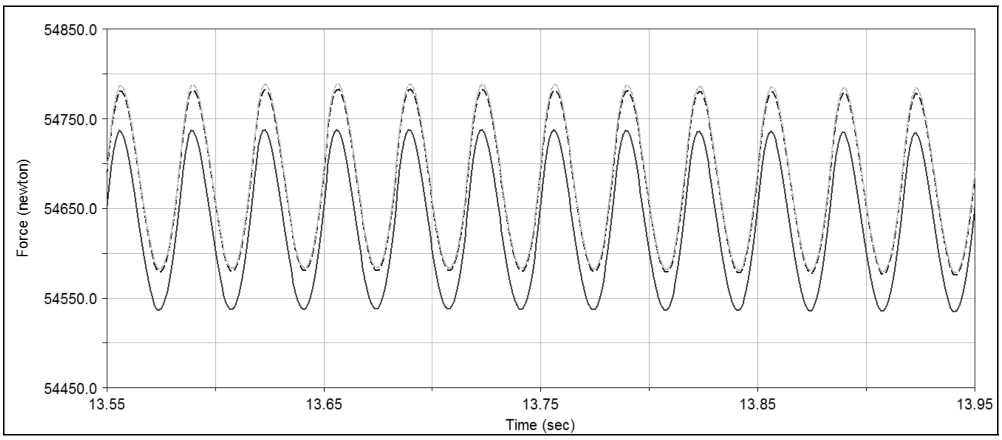

Figure 8: Contact force on tangent track at 18 m/s. Solid line: *average track*, Dashed line: *soft ballast*, Dotted line: *soft pad*.

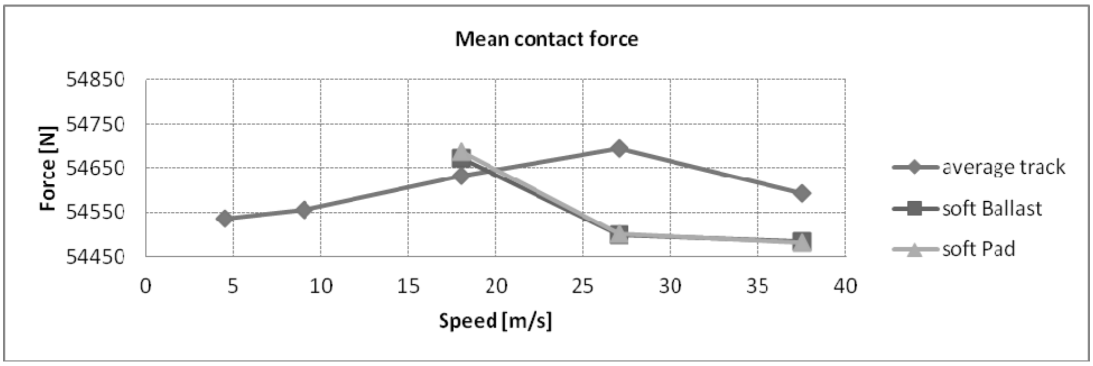

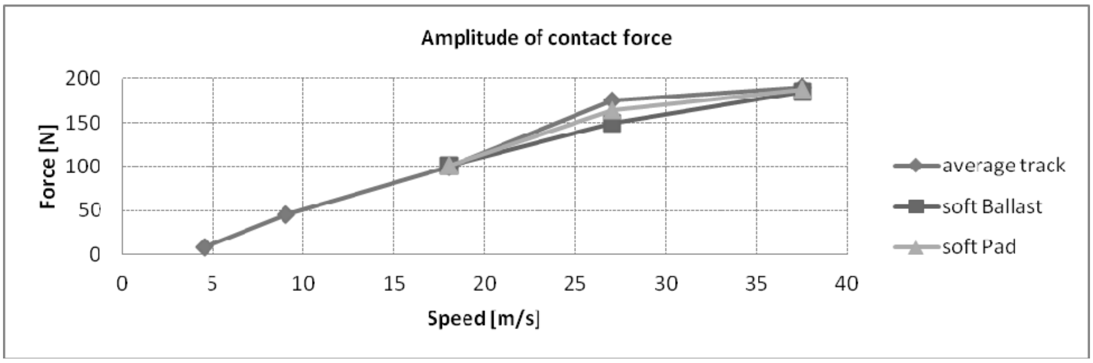

Figure 9: Average (above) and dynamic amplitude (below) of the wheel-rail contact force at different speeds and with different pad or ballast stiffness.

4.2 Effects of speed on the sleeper reaction force

In this paragraph the effect of speed on the sleeper reaction force is shown. In the case of the *average track* in the analysed speed range (4.5-37.5 m/s, i.e. 16.2-135 km/h, that is representative from shunting to a conventional main line speed), a correction of the measured force should be made, taking into account the dynamic effects of the train speed.

It can also be observed that that there is a “dynamic interaction” between the two consecutive wheels of a bogie, being the effect of the speed greater on the trailing wheel (*wheel 2* in the figures). Figure 10 shows the effect of the speed on the total strain signal for the case of the *average track*.

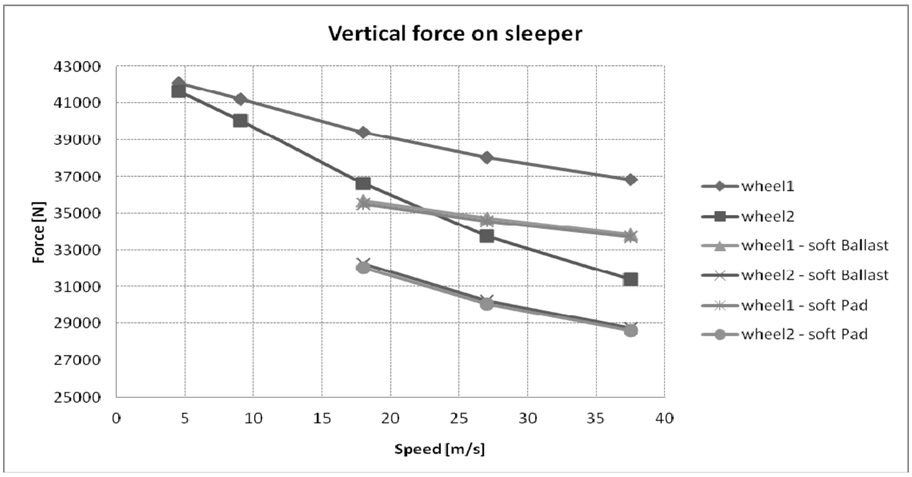

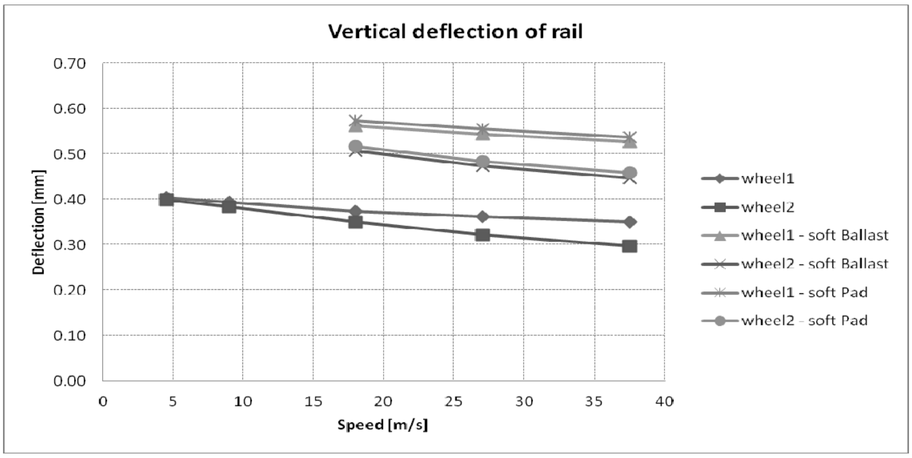

Figure 10: Effect of speed on sleeper reaction force (above) and on rail total displacement (below). Higher curves are relative to *average track,* lower curves are relative to *soft pad* (k_{pv}=50 kN/mm) or *soft ballast* (k_{bv}=80 kN/mm) conditions.

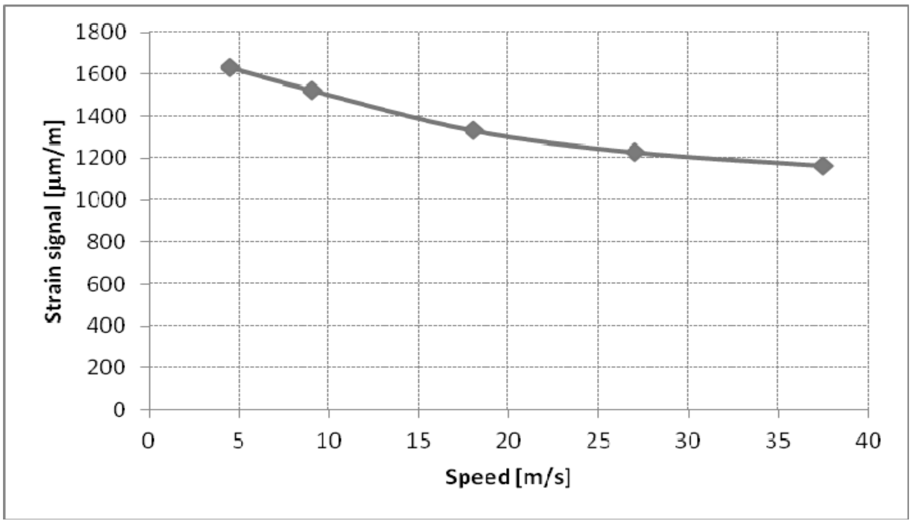

Figure 11: Effect of speed on the total strain signal for the average track.

4.3 Effects of stiffness on sleeper reaction force

The effect of a uniform change in the track stiffness, i.e. that found in the *soft pad* and *soft ballast* models, vs. the *average track* is visible in Figure 10 above; quite obviously the uniform reduction of stiffness results in the distribution of the wheel load on more sleepers reducing at the same time the reaction under each single sleeper.

This latter was analysed, introducing result from multibody simulations in the "dynamic" finite elements model and trying to quantify the influence of that reduction in terms of strain signal measured by the sensors.

From Figure 12 it can be seen that total strain signal is not much influenced by the reduction of the track stiffness at the first two of the considered speed, while at the higher speed there is instead a significant reduction of the strain signal. The small influence of the total track stiffness at lower speeds was confirmed by the use of the static finite element model as shown in Figure 13.

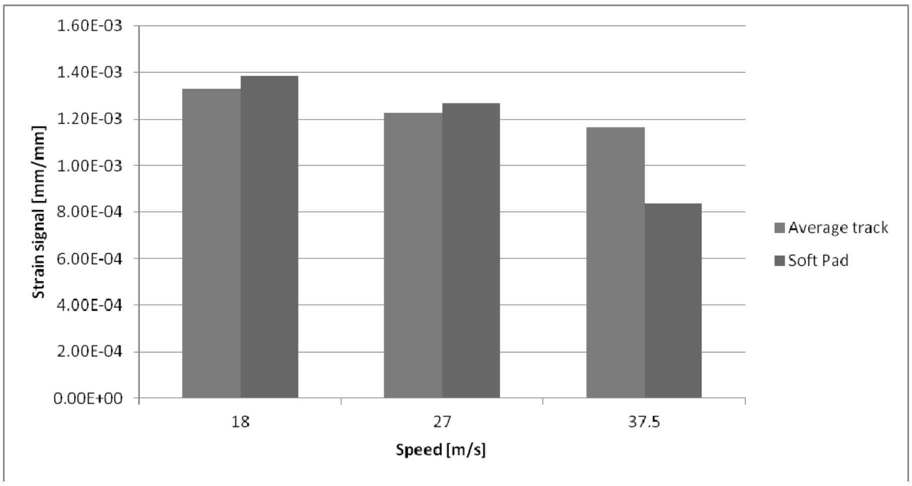

Figure 12: Comparison of strain recorded by the sensor for the *average track* and the *soft pad* cases as computed by the dynamic model for three different speeds.

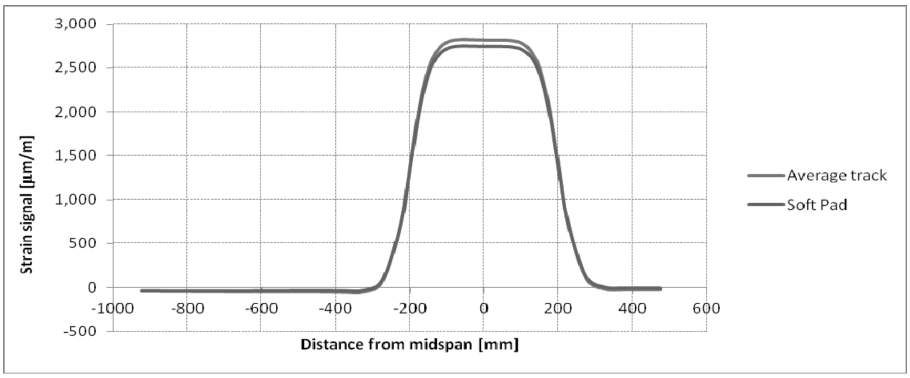

Figure 13: Effect of pad stiffness reduction from k_{pv}=150 kN/mm (*average track*) to k_{pv}= 50 kN/mm (*soft pad*) on total strain signal with a static load.

4.4 Effects of local ballast stiffness reduction

The last case simulated was the system (and sensor signal) behaviour in response to the poor tamping of a single sleeper. This case can be quite frequent where track superstructure is not uniform as a result, for example, of water drainage problem.

The intention of the simulation was to assess the response of a measuring system made of the sensor in case the support to an instrumented track is locally impaired or completely lost. Poor tamping was therefore modelled with a local reduction of ballast stiffness from k_{bv}=160 kN/mm to 16, 3.2 or 0.8 kN/mm. Results are shown in Figure 14 from which the effect of quite evident.

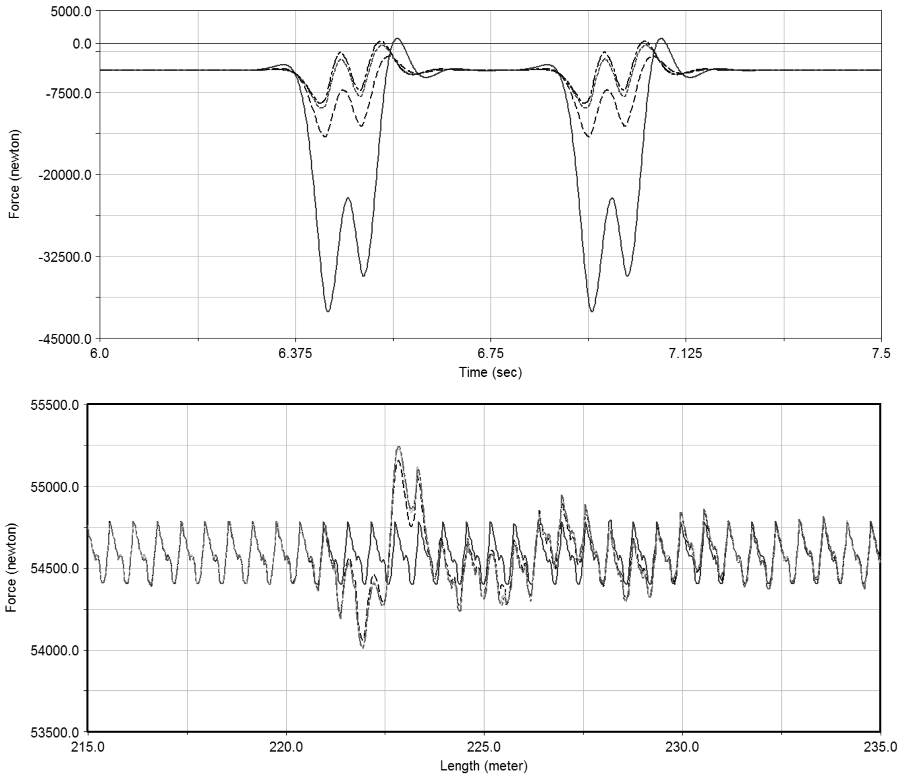

Figure 14: Force on sleeper (above) and wheel-rail contact force (below) with different vertical ballast stiffness simulated at a speed of 37.5 m/s. Solid line: *average track*, Dashed line: 16 kN/mm, Dotted line: 3.2 kN/mm, Dash-dotted line: 0.8 kN/mm.

The detrimental effect of poor tamping of a sleeper is better explained by considering the ratio of the peak sleeper force with respect to that pertinent to the homogeneous track case. Figure 15 shows that the effects of such defect are visible, in the worst case, up to three metres from the defective sleeper support.

This analysis allows to find which is the minimum still tolerable distance where a defective ballast tamping can be found or, stated differently, which is the minimum distance *beyond* the measuring system that should be correctly and uniformly tamped.

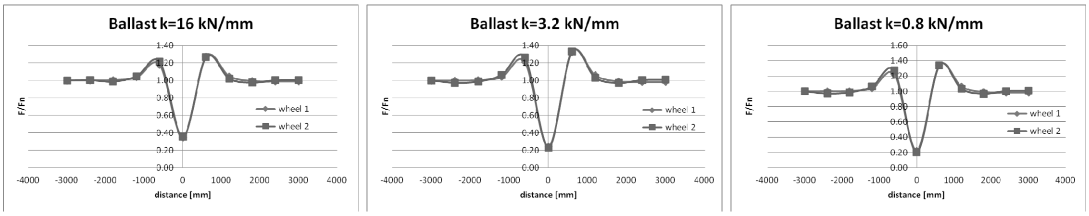

Figure 15: Distance influenced by a single poorly tamped sleeper in the cases of k_{bv}=16 kN/mm (left), 3.2 kN/mm (centre) and 0.8 kN/mm (right) ballast vertical stiffness.

5 Conclusions and developments

In this paper the *Flextrack* tool of the *VI-Rail* multibody software was used in order to understand the effect of varying track stiffness and vehicle speed on the sleeper reaction force. Multibody simulation results were used as input for a finite element model in order to evaluate the behaviour of a wheel-rail contact force transducer. Results are complete and are presented only for the case of tangent track where vertical forces are present, while further simulations are currently in progress to complete the evaluation also in the curved track case and the resulting presence of lateral forces.

Results show that, even for just the tangent track case, a correction on the strain signal produced by the sensors should be made to compensate for the effect of the speed, and that at higher speeds attention should also be paid at the interaction of two subsequent wheels.

Moreover the simulations show that the effect of the global track stiffness allows for a certain tolerance to this parameter as long inasmuch its variations can be accepted without compromising the functionality of the transducer.

The effect of a single “poor tamping of a sleeper” defect was analysed giving an indication on the length of track that should be kept in good conditions around the transducer installation.

It can be concluded that the combination of the methodology which combines the use of an advanced multibody simulation and a detailed finite element analysis is a powerful tool to assess the robustness of any wheel-rail measuring system, including the one proposed and installed by the authors.

References

[1] A. Bracciali, R. Ciuffi, F. Piccioli: "Progetto e validazione di un sensore estensimetrico multifunzione per il binario ferroviario", XXX Convegno AIAS, Alghero, 12-15.9.2001, 901-912 (in Italian).

[2] A. Bracciali, P. Folgarait: “New Sensor For Lateral & Vertical Wheel-Rail Forces Measurements”, Proceedings of Railway Engineering 2004 Conference, London, 6-7 July 2004.

[3] L. Di Benedetto, A. Bracciali, T. De Cicco, F. Piccioli: “Diagnosi delle condizioni di marcia di un rotabile con un sistema di misura delle forze laterali e verticali al contatto ruota-rotaia”, AIAS – Associazione Italiana per l’Analisi delle Sollecitazioni, XXXIX Convegno Nazionale, 7-10 settembre 2010, Maratea (in Italian).

[4] Y. Bezin, S.D. Iwnicki, M. Cavalletti, E. deVries, F. Shahzad, G. Evans: "An investigation of sleeper voids using a flexible track model integrated with railway multi-body dynamics", JRRT 276, Proc. IMechE Vol. 223 Part F: J. Rail and Rapid Transit, 597-607.

[5] EN 13674-1:2003+A1 (2007). “Railway applications - Track - Rail - Part 1: Vignole railway rails 46 kg/m and above”.